JOC The Journal of Organic Chemistry

Article

pubs.acs.org/joc

Influence of Substituent and Benzoannulation on Photophysical Properties of 1-Benzoylmethyleneisoquinoline Difluoroborates

Borys Ośmiałowski,*[,†] Anna Zakrzewska,[†] Beata Jędrzejewska,[†] Anna Grabarz,[‡] Robert Zaleśny,[‡,§] Wojciech Bartkowiak,[‡] and Erkki Kolehmainen[∥]

[†]Faculty of Chemical Technology and Engineering, UTP University of Science and Technology, Seminaryjna 3, PL-85326 Bydgoszcz, Poland

[‡]Faculty of Chemistry, Wrocław University of Technology, Wyb. Wyspiańskiego 27, PL-50370 Wrocław, Poland

[§]Division of Theoretical Chemistry and Biology, School of Biotechnology, Royal Institute of Technology, SE-10691 Stockholm, Sweden

[∥]Department of Chemistry, University of Jyväskylä, P.O. Box 35, FI-40014 Jyväskylä, Finland

Supporting Information

ABSTRACT: A series of 1-benzoylmethyleneisoquinoline difluoroborates were synthesized, and their photophysical properties were determined. The effect of the substituent and benzoannulation on their properties was investigated to make a comparison with recently published results focused on related quinolines. The photophysical properties of isoquinoline derivatives differ from those of quinolines, and the most pronounced differences are found for the fluorescence quantum yields. Both experimental and theoretical approaches were used to explain the observed photophysical properties.

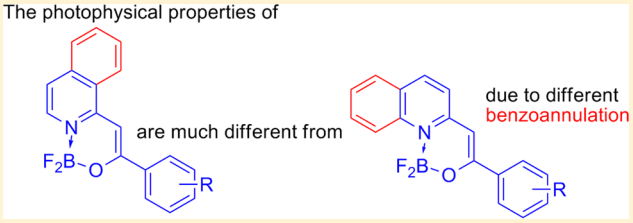

INTRODUCTION

Dyes carrying the BF_2 moiety are known to be fluorescent. Among them, the most common group are the BODIPY dyes.[1−3] Although a plethora of studies were devoted to BODIPYs, these dyes are still in the limelight. The intense studies concern not only their absorption and fluorescence properties but also electrogenerated chemiluminescence, for example.[4] However, studies of the BF_2-carrying fluorescent dyes different from BODIPYs are rare. Very recently, the first survey on these molecules was published by Ziessel et al.[5] Moreover, there are some attempts to clarify their properties by computational approaches.[6−8] Thus, there is still a need to investigate how their properties can be tuned in order to obtain desired photophysical characteristics. This is especially important for fluorescence microscopy,[9] anion sensing applications[10,11] or biolabeling,[12] photodynamic therapy,[3] and solar cells[13,14] to name a few. The compounds studied now contain the NBF_2O moiety.[15−21] In the literature there exist reports on compounds where the BF_2-group is chelated also symmetrically in NBF_2N[22−25] and OBF_2O[26−29] moieties. Also, molecules carrying the NBF_2O fragment, especially imines based on hydroxyl-containing Schiff bases, are known.[30−33]

Tailoring molecular properties by a relatively simple synthetic procedures is highly desirable. Systematic change of a substituent may be a successful route in many instances. However, benzoannulation may also possess a crucial role in the case of π-conjugated molecules,[34−39] where it is known to have a fundamental impact (qualitative and quantitative) on the properties of compounds exhibiting tautomerism, for example, in heterocyclic ketones.[37,40−43] Presumably, the properties of BF_2-carrying molecules may also be tuned in this way. This is due to the fact that the proton involved in intramolecular hydrogen bonding[40,41] can be easily replaced by another acid such as the BF_2^+ cation. The proton-to-BF_2 exchange thus creates an opportunity to synthesize a number of new dyes. There are several publications on benzoannulation of the BODIPY core and its influence on the photophysical properties of these molecules.[44−48] This was the inspiration to study the isomers of 2-benzoylmethylenequinoline difluoroborates studied by us recently,[49] *id est*, the 1-benzoylmethyleneisoquinoline derivatives. It is worth mentioning that the effect of π-electron conjugation on the fluorescence quantum yield was studied on model compounds.[50] However, to the best of our knowledge, no detailed studies are presented on the effect of structural isomerism on the photophysical properties of BF_2-carrying molecules. This leads to a hypothesis that both the length and the conjugation route should be taken into account when designing fluorescent molecules. Chart 1 depicts 1-benzoylmethyleneisoquinoline difluoroborates and their numbering. The synthesis of the parent 1-benzoylmethyleneisoquinolines was performed as described elsewhere for similar compounds.[51] The conversion of these substrates into fluorescent BF_2-carrying molecules was performed as in an earlier study.[49,52]

Received: September 30, 2014
Published: January 29, 2015

DOI: 10.1021/jo502244j
J. Org. Chem. 2015, 80, 2072−2080

Chart 1. Reaction Scheme and Structures in 1-Benzoylmethyleneisoquinoline Difluoroborates

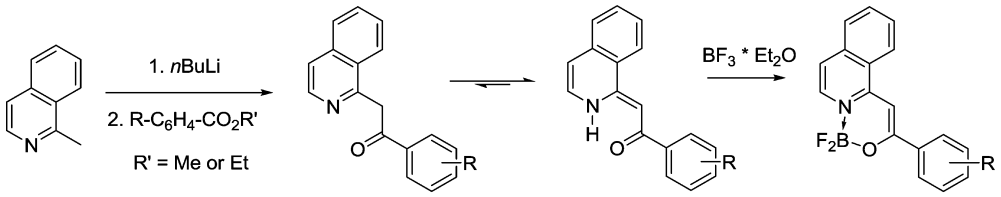

R = 4-NMe_2 (**1**), 4-OMe (**2**), 4-Me (**3**), 3-Me (**4**), H (**5**), 4-Br (**6**), 3-Br (**7**), 4-CF_3 (**8**)

RESULTS AND DISCUSSION

Linear Photophysical Properties. The photophysical properties of compounds **1**–**8** (Chart 1) were studied in chloroform. This solvent is known to prevent boron–ligand dissociation, exciplex formation, or the photochemical reactions possible in solvents containing Lewis bases, aromatic rings, or double bonds.[53] Moreover, self-aggregation is not preferred in dilute solutions as has already been demonstrated for quinoline derivatives.[49] Figure 1 shows the absorption spectra of **1**–**8**,

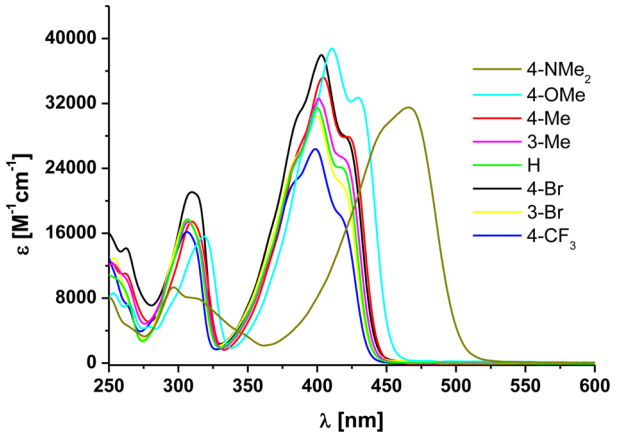

Figure 1. Electronic absorption spectra of **1**–**8** in $CHCl_3$.

and the corresponding values are presented in Table 1. The molecules show absorption spectra in solution characterized by two distinct bands, the main band existing within the range 330–500 nm depending on the substituent and the second band at about 300–320 nm. Absorption spectra of complexes **2**–**8** exhibit fine structure, although it is not as distinct as in quinoline isomers, whereas **1** exhibits an almost structureless band with a maximum close to 460 nm. Additionally, all eight complexes have high extinction coefficients (26400–38800 $M^{-1}cm^{-1}$), which is typical for $\pi \rightarrow \pi^*$ transitions (Figure 1). Except for **1**, the shape of the absorption spectra remains very similar to that of the parent compound (R=H), and it is dependent on the electron-withdrawing or electron-releasing group at different positions in the phenyl ring. The absorption maximum and its intensity, however, differ among the studied set of compounds.

In order to evaluate the effect of the different substituents on the linear optical properties, $-CF_3$ was used as a benchmark acceptor group, as this moiety is the strongest acceptor in the series. In comparison with others, **8** (4-CF_3) shows a similar but blue-shifted and less intense absorption band. Absorption at λ_{max} was found to progressively shift to longer wavelength upon replacing this substituent by weaker electron-withdrawing (Br) and then electron-releasing (4-Me, 4-OMe, and 4-NMe_2) substituents (Table 1). This effect was accompanied by an increase of the absorption intensity. A considerable red shift of the major absorption band was observed for compound **1** (4-NMe_2) (Figures 1–2). The 4-NMe_2 substituent causes a 66 nm red shift in absorption relative to the parent compound **5**. This result indicates that the absorption arises from polarized π–π^* transition in the NMe_2 substituted molecule. The character of this transition will be discussed in more detail in the subsequent section. The significant density reorganization upon excitation was prevented after the addition of gaseous HCl into the measurement cell (Figure 2) and formation of the 4-NMe_2H^+ cation. The absorption maximum of the 4-NMe_2H^+ derivative was blue-shifted when compared with the free base and the unsubstituted congener (**5**). Similar to another report,[49] this reveals that the 4-NMe_2H^+ group has weak electron-acceptor properties, which is in agreement with its cationic character. This effect retracts after the addition of gaseous ammonia to a solution of protonated **1**. A similar effect was observed for 2-

Table 1. Photophysical Data[a] for Compounds 1–8

no.	substituent	λ^{ab}_{max} / ε*10^4	λ^{Fl}_{max}	$\Delta\nu^1$	$\Delta\nu^2$	ϕ_{Fl}	τ_1 / α_1	τ_2 / α_2	τ_{av}	χ^2	k_r	k_{nr}
1	4-NMe_2	466 3.15	512.4	1943[b]		0.743	458 4.33	2427 95.67	2341.7	1.83	3.17	1.10
2	4-OMe	410.5 3.88	478.2	1320	3449	0.313	405 15.75	1061 84.25	957.7	1.29	3.26	7.18
3	4-Me	404 3.52	471	1113	3521	0.087	348 92.82	747 7.18	376.7	1.28	2.32	24.23
4	3-Me	401.5 3.26	464.8	1077	3392	0.060	242 98.27	825 1.73	252.1	1.17	2.37	37.30
5	H	400 3.14	463.2	1139	3411	0.046	191 98.77	1109 1.23	202.3	1.16	2.28	47.15
6	4-Br	403 3.80	466.4	1118	3373	0.049	211 98.19	1374 1.81	232.1	1.12	2.10	41.00
7	3-Br	399.5 3.05	465	1082	3526	0.033	154 97.33	1249 2.67	183.2	1.50	1.82	52.76
8	4-CF_3	398.5 2.64	464.6	1092	3570	0.026	127 98.63	1053 1.37	139.7	1.20	1.88	69.71

[a]Absorption (λ^{ab}_{max}; nm), fluorescence maxima (λ^{Fl}_{max}; nm), shift ($\Delta\nu$, cm^{-1}), maximum extinction coefficient (ε; $M^{-1}cm^{-1}$), fluorescence quantum yield (ϕ_{Fl}), fluorescence lifetime (τ; ps), their amplitudes (α) and correlation coefficients (χ^2),and radiative (k_r; 10^8 s^{-1}) and nonradiative (k_{nr}; 10^8 s^{-1}) rate constants. [b]The difference between positions of the band maxima of the absorption and emission spectra of 4-NMe_2.

DOI: 10.1021/jo502244j
J. Org. Chem. 2015, 80, 2072–2080

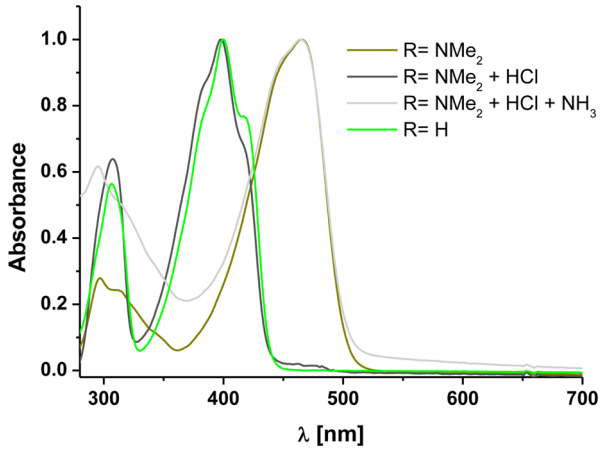

Figure 2. Comparison of the electronic absorption spectra of the parent compound (**5**), 4-NMe_2 (**1**) derivative, and its HCl salt (**1** + HCl) neutralized with gaseous ammonia (**1** + HCl + NH_3).

benzoyl(4-dimethylamino)methylenequinoline difluoroborate.[49]

Likewise, the emission spectra and fluorescence lifetimes of **1**−**8** were measured in chloroform. The results are given in Figure 3 and Table 1. All compounds exhibit fluorescence

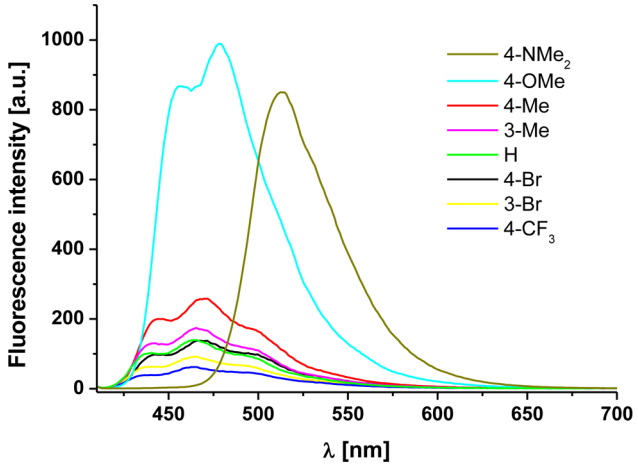

Figure 3. Fluorescence spectra of **1**−**8** (3−4 [μM]) in $CHCl_3$. λ_{ex} = 404 nm.

ranging from the blue to green region. Figure 3 compares the parent compound (R═H) with its derivatives containing electron-withdrawing and electron-donating groups to explore substituent effects on fluorescence spectra. As for the absorption spectra of **1**−**8**, decreasing accepting strength and increasing donating ability of the substituent result in stronger and red-shifted emission. Among them, **1** and **2** exhibit the strongest fluorescence, whereas the weakest emission occurs for the complex containing the 4-CF_3 substituent. However, the fluorescence of **1** (4-NMe_2) is different from that of the others because the emission spectra of **1** show an unstructured band (the corresponding Stokes shift is 1943 cm^{-1}). The same is observed in many other compounds including BODIPY dyes after the introduction of a strong electron-donating amino group.[54−58]

A mirror symmetry holds between the absorption and emission spectra as shown in Figure 4 (for compound **5**, the remaining spectra are given in Supporting Information) suggesting a weak structural relaxation of the Franck−Condon singlet excited state.

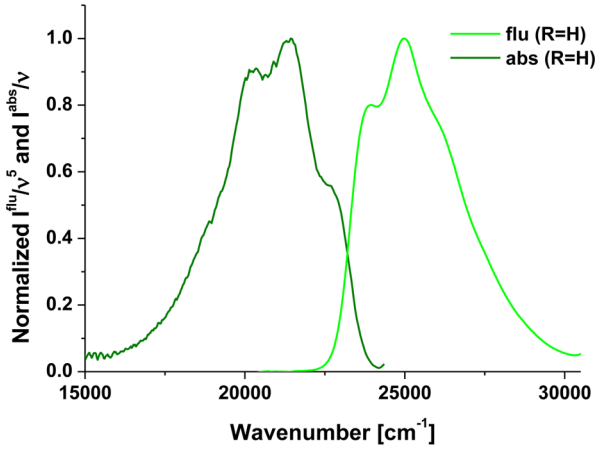

Figure 4. Normalized and scaled[59,60] electronic absorption and fluorescence spectra of **5** in $CHCl_3$.

The fluorescence quantum yield was determined relative to the coumarine 1 quantum counter (ϕ_{ref} = 0.64) with excitation at 404 nm. Derivatives **1** and **2** exhibit good fluorescence quantum yield (0.74 and 0.31), whereas for the others, it is lower by 1 order of magnitude.

Figure 5 shows the biexponential fluorescence decay curve for **5**. The same is used for the fitting of other derivatives. An

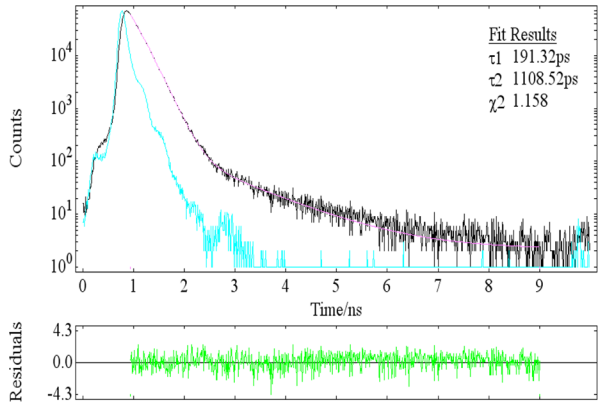

Figure 5. Fluorescence decay curve for **5** recorded in $CHCl_3$; λ_{ex} = 404 nm; λ_{em} = 450 nm.

additional long-lived component that appeared in these compounds suggests a complex photophysical process. The fluorescence lifetimes measured by a time correlated single photon counting method are shown in Table 1 above.

In the parent compound (**5**), ϕ_{Fl} and τ_{Fl} are 0.046 and 191 ps (major component), respectively. These values are diminished to 0.026 and 127 ps, respectively, when the 4-CF_3 group is present (**8**). Hence, the rate constant of radiative k_r deactivation is decreased from 2.28 × 10^8 to 1.82 × 10^8 s^{-1}, respectively, caused by the strong electron-withdrawing character of the substituent. However, introducing an electron-releasing substituent enhances the fluorescence quantum yields, lifetimes, and Stokes shift, e.g., for 4-NMe_2, ϕ_{Fl} = 0.74, τ_{Fl} = 2427 ps (major component of different nature than that in **3**−**8**; see Table 1 for τ_1 and τ_2), and $\Delta\nu$ = 1943 cm^{-1}. Both ϕ_{Fl} and τ_{Fl} show the monotonous increase with the increase in electron-

DOI: 10.1021/jo502244j
J. Org. Chem. 2015, 80, 2072−2080

Table 2. Calculated Spectroscopic Parameters Corresponding to the Lowest Lying ($\pi \rightarrow \pi^*$) Excited State Where λ_v and λ_{ad} Correspond to the Vertical and Adiabatic Transitions

	functionals									
	B3LYP			CAM-B3LYP			PBE0			
substituent (compd)	λ_v [nm]	λ_{ad} [nm]	f	λ_v [nm]	λ_{ad} [nm]	f	λ_v [nm]	λ_{ad} [nm]	f	exp λ_{0-0} [nm]
4-NMe_2 (**1**)	460	477	0.985	394	430	1.118	422	438	1.042	491
4-OMe (**2**)	412	437	0.896	367	411	0.955	398	424	0.920	442
4-Me (**3**)	401	440	0.812	360	395	0.858	388	423	0.830	438
3-Me (**4**)	396	426	0.744	360	397	0.817	385	415	0.764	431
H (**5**)	395	426	0.726	356	390	0.781	383	413	0.745	429
4-Br (**6**)	400	438	0.856	359	397	0.889	388	423	0.875	432
3-Br (**7**)	395	438	0.743	356	393	0.798	386	414	0.780	430
4-CF_3 (**8**)	397	432	0.739	355	393	0.789	384	418	0.745	427

donating abilities of the substituent. Additionally, the data compiled in Table 1 show that for tested compounds the nonradiative transition rates are of the same order as the radiative ones only for **1** and **2**. In the case of others, the nonradiative transition rates are at least 1 order of magnitude larger than the radiative ones, which indicates contribution of the excited singlet state that deactivates by the internal conversion processes.

The complexes studied here can be grouped into two categories. One includes compound **1** that is characterized by rather large Stokes shifts with long radiative lifetimes and low-energy emissions and **2**−**8** that have the high-energy emissions and short fluorescence lifetimes. This suggests that emissions arise from different types of excited states. Presumably, an increase in π conjugation length typically results in a red shift of emission and change in corresponding quantum yield.[50] The spectra roughly follow this rule, but some exceptions were also observed. For example, the donating substituent carrying a lone-electron pair as in **1** extends the electron conjugation with respect to that in **5**. Moreover, this allows efficient polarization of the electronic density upon excitation leading to the largest red-shifted emission. However, the length of conjugation is not the only parameter that influences the emissive state energy of the complexes. The inductive effects or mentioned charge transfer should be also taken into account.

As stated above, the distinct red features in the absorption spectrum for **1** are ascribed to substantial density changes in the π−π^* excited state. These features are dominated by excitations in which charge is transferred from donor (4-NMe_2) to the acceptor (NBF_2O) moiety. These observations further support the same interpretation for the 4-OMe derivative (**2**) where reorganization of electron density is less efficient than that in **1**. From the fluorescence spectra, the emission maximum of **1** is red-shifted by 34 nm compared to that for **2**. Although the electron-donating 4-OMe does not seem to make such a significant effect as 4-NMe_2, the radiative lifetimes follow the expected trend showing some differences in the quantum yield and fluorescence decay. For **1**, τ_2 is more than twice the value for **2**, indicating a large long-lived contribution coming from the effect of the strong electron-donating group. The more electron-rich **1** (versus **5**) may slightly weaken the acceptor ability of the NBF_2O moiety, thus increasing the energy of the transition. Within all **1**−**8**, where $\pi \rightarrow \pi^*$ transitions dominate the electronic transitions, the 4-OMe exerts a subtle but measurable effect on fluorescence decay, whereas the 4-NMe_2 has a significant effect on the excited-state properties.

The obtained results suggest that there may be two excited-state conformers for these compounds. One has a structure conducive to the $\pi \rightarrow \pi^*$ state being lowest energy in the excited state and gives rise to a short-lived (127−458 ps) $\pi \rightarrow \pi^*$ fluorescence. The structure dominates for 1-benzoylmethyleneisoquinoline difluoroborates bearing electron-withdrawing substituents and a weak electron-releasing group. Its share of average fluorescence lifetime is in the range 99−93%. In the case of compounds containing a strong electron-donor (4-NMe_2), the dominant structure gives a transition associated with substantial charge reorganization and is the source of the much longer-lived emission (2.5 ns). While one could expect the systematic changes of properties related to the substituent alteration, here a sudden drop of properties is observed when passing from 4-Me via 4-OMe to 4-NMe_2. This suggests the existence of substances with two very different fluorescence character in the latter derivative. A possible scenario is that a conformer with the twisted NMe_2 group (or $C_6H_4NMe_2$) exists.[61−63] The excited-state geometry optimization of 4-NMe_2 (at the CAM-B3LYP/6-311++G(d,p) level of theory) revealed the existence of a stable conformer with the NMe_2 group coplanar with phenyl ring. The calculated Stokes shift (48 nm) was found to be in excellent agreement with the experimental value (46 nm).

In summary, the intensity of the absorption and emission bands increases with increasing electron-donating properties of the substituent in the phenyl moiety, and the maxima of the bands are red-shifted. A greater disparity in the electron-donating ability of the 4-NMe_2 group seems to result in a stronger transition with charge reorganization dominated by the more electron-rich aryl group. However, the $\pi \rightarrow \pi^*$ transitions dominate for other 1-benzoylmethyleneisoquinoline difluoroborates.

Comparisons of Isoquinolines with Quinolines. For comparison purposes and in order to gain further insight into the properties of **1**−**8**, a series of charts were drawn (Supporting Information). The properties of 2-benzoylmethylenequinoline difluoroborates were used for these purposes.[49] These comparisons allow one to draw the following conclusions for the NMR-derived data: (a) the ^{15}N chemical shift (sensitive to the environment[64]) is linearly dependent (correlation coefficient R = 0.99, **5** and **8** excluded) on the substituent constant with a similar slope between the series but a different intercept (Chart S1, Supporting Information); and (b) the same applies for other chemical shifts as, for example, ^{19}F data (R = 0.90, **1** excluded from correlation), ^{13}C of carbon no. 1 in isoquinoline (R = 0.98), CO (R = 0.95), and methine CH carbon (R = 0.95) atoms. For the photophysical data, it can be concluded that (a) the fluorescence quantum yields are, in

DOI: 10.1021/jo502244j
J. Org. Chem. 2015, 80, 2072−2080

Table 3. Kohn-Sham Frontier Orbitals Determined Using the B3LYP Functional and the 6-311++G(d,p) Basis Set at the Contour Surfaces of Orbital Amplitude 0.04 e/bohr^3

Compound	HOMO	LUMO
1 (4-NMe_2)	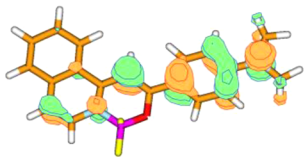	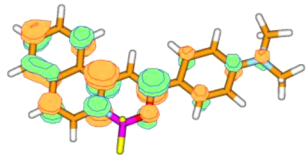
5 (H)	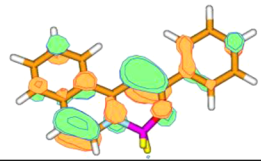	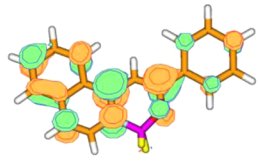

general, higher for quinoline derivatives than that for isoquinolines (Chart S2, Supporting Information); (b) the data of the radiative and nonradiative rate constants suggest the nonradiative mechanism dominates (Chart S3, Supporting Information) and is responsible for much lower fluorescence quantum yield (Chart S4, Supporting Information) in isoquinolines, and that (c) for the fluorescence lifetimes, the opposite effect is observed between short and long-lived species, *id est*, the correlation with the substituent constant is observed for short lifetimes in isoquinolines (R = 0.93) and for long lifetimes for quinolines (R = 0.97, Chart S6, Supporting Information). The above-mentioned observations lead to the conclusion that variable benzoannulation causes dramatic changes in the photophysical properties of the studied molecules. One mechanism that can cause a sudden drop in the fluorescence quantum yield is high nonradiative processes caused by vibrations of the molecular skeleton or by much stronger interaction of the BF_2 moiety with the solvent molecules (compare the topology of these derivatives). The detailed studies on these effects are in progress.

Quantum Chemical Calculations. In order to support experimental data, the quantum chemical calculations were performed. In particular, one of the primary aims behind these computations was to analyze the vibrational fine structure of the absorption band related to the lowest-lying $\pi \rightarrow \pi^*$ transition and the associated changes in electronic density. The oscillator strength (f) accompanying this transition is rather large for all studied molecules and is presented in Table 2. It should be highlighted that the largest probability was observed for the one-electron HOMO → LUMO excitation. The frontier orbitals involved in the $\pi \rightarrow \pi^*$ transition for **1** and **5** are shown in Table 3 (a complete data set for all molecules is presented in Experimental Section). As seen in accordance with previous conclusions based on experimental data, much more significant density change upon excitation is found for 4-NMe_2 substituent. In order to put these changes on a quantitative basis, the fragment analysis of frontier molecular orbitals involved in the excitation was performed (Supporting Information). It follows from this analysis that the net charge transferred from fragment **B** to fragment **A** (Figure 6) upon excitation is 0.47e and 0.045e for compounds **1** and **5**, respectively.

Although the comparison of computed vertical excitation energy with experimental absorption band maxima still remains the most common route, critical assessment of this approach has already been performed by some authors.[65−67] In Table 2, there is presented the wavelength corresponding to vertical

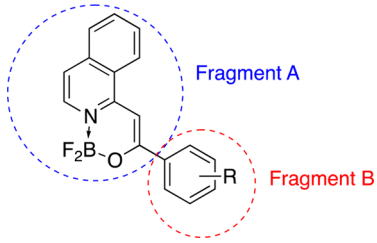

Figure 6. Scheme of the decomposition of the molecule into fragments.

excitation (computed without zero-point vibrational energy included) and wavelength related to the adiabatic transition (within the IMDHO model, the latter value corresponds to the 0−0 excitation). The results clearly show that the B3LYP functional provides the most accurate estimation of experimental absorption/fluorescence crossing point (referred to as 0−0 energy). The other two functionals significantly overestimate the 0−0 energy; the largest deviation from experimental data is found for compound **1**, characterized by significant charge reorganization upon excitation. Other groups have reported the accurate estimation of the spectroscopic parameters (within the TD-DFT scheme) for the cyanine-like molecules (such as BODIPY).[68−73]

In order to gain insight into the structure of experimentally recorded absorption bands, we have also performed a simulation of their vibrational fine structure. The results are presented in Figures 7 and 8. In the case of all performed simulations, the homogeneous broadening was set to 100 cm^{-1}, and standard deviation of the distribution of 0−0 excitation energies corresponding to inhomogeneous broadening was chosen as 420(**6**), 450(**2**, **3**, **5**, 7, **8**) 475(**4**), or 500 cm^{-1}(**1**) to correctly reproduce the overall absorption band shapes. As can be seen in Figure 7, among three employed functionals, only CAM-B3LYP satisfactorily predicts the vibrational fine structure of the absorption band corresponding to the $\pi \rightarrow \pi^*$ transition. Two other functionals incorrectly determine the intensity ratio for major band shoulders. Within the framework of the applied model, it can be directly related to the displacements between the potential energy surfaces, which are computed based on the excited-state gradients. The differences between the experimental band shape and the profiles simulated using B3LYP and PBE0 functionals may indicate, indirectly, that the latter two functionals have difficulties in predicting excited-state gradients. Thus, the CAM-B3LYP functional was used to simulate the band shapes

DOI: 10.1021/jo502244j
J. Org. Chem. 2015, 80, 2072−2080

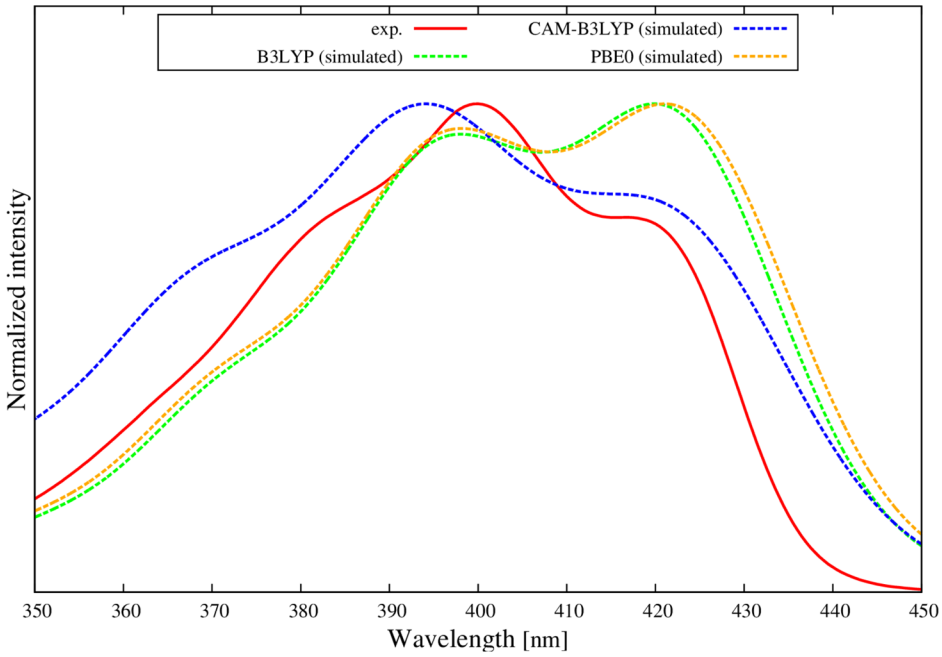

Figure 7. Comparison of experimental and simulated absorption spectra for the R═H derivative. The spectra were shifted to match the experimental long-wavelength feature.

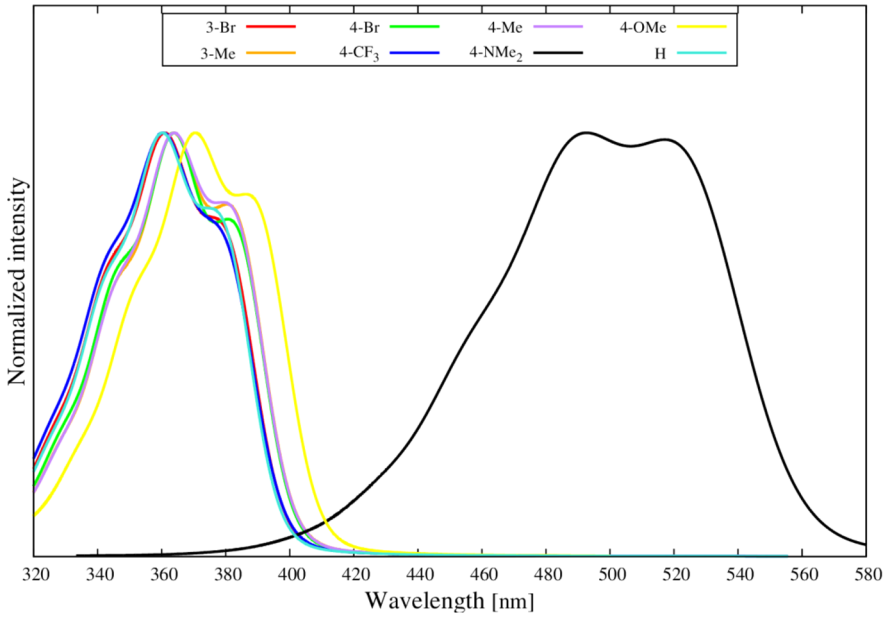

Figure 8. Absorption spectra simulated using the CAM-B3LYP functional.

for all series of compounds (cf. Figure 8), which are in good accordance with the experimental spectra presented in Figure 1.

■ CONCLUSIONS

The spectral and computational data show that the absorption and fluorescence properties of substituted 1-benzoylmethyleneisoquinoline difluoroborates are similar to those in quinoline derivatives, while some small spectral shifts are noticed. The most dramatic differences between quinoline and isoquinoline derivatives are within their fluorescence quantum yield, which decreases quickly when going from strong to weak electron-donating substituents. This shows that isoquinolines are less attractive for their use as fluorescent probes. Moreover, this also shows that special care should be paid not only to the substituent applied, degree of π-electron conjugation, and benzoannulation but also to the way benzoannulation takes place. This clearly influences the synthetic procedures that would lead to materials with desired properties. The correlations of the NMR chemical shifts with substituent constants are similar to those in in quinolines making the substituent effect in the ground state similar between these series. It has been found that only CAM-B3LYP functionals yields the correct absorption band shape for the studied molecules.

DOI: 10.1021/jo502244j
J. Org. Chem. 2015, 80, 2072−2080

EXPERIMENTAL SECTION

The 1-benzoylmethyleneisoquinoline difluoroborates were synthesized as before (ketone synthesis;[51] complexation[22]). The same applies for visible[49] and NMR[52] spectral measurements. Electronic structure calculations were performed using the Kohn−Sham formulation of the density functional theory. In order to take into account the conditions of experimental measurements, the calculations were carried out in the presence of the solvent, using the linear response polarizable continuum model (LR-PCM[74]). Comparison of LR-PCM with more accurate corrected LR-PCM can be found in a recent paper by Chibani et al.[75] Optimization of the ground-state geometry was carried out using three different exchange-correlation functionals: B3LYP, CAM-B3LYP, and PBE0. Vertical excitation energies were computed employing time-dependent density functional theory. For all quantum chemical calculations, the 6-311++G(d,p) basis set was used. All electronic structure calculations were performed using the Gaussian 2009 D01 program.[76] Additionally, in order to simulate the vibrational structure of the absorption spectra, the *orca_asa* program was used (a part of ORCA package).[77] Simulations of the absorption bands, interrelated with transitions to the (π−π^*) excited state, were performed using independent mode displaced harmonic oscillator (IMDHO) approximation. In the case of the ground electronic state, the entire set of normal modes of vibration was included in simulations. Dimensionless normal coordinate displacements ($\Delta_{Q,k}$) for the excited state with respect to the ground-state equilibrium geometry were calculated using custom software as follows:

$$\Delta_{Q,k} = -\frac{1}{\omega_{ek}^2}\left[\frac{\partial E}{\partial Q_k}\right]_{Q=0}$$

where $[\partial E/\partial Q_k]_{Q=0}$ corresponds to the excited-state potential energy gradient along the k-th normal mode at the ground-state geometry. The energy of adiabatic transition was computed according to the following formula:

$$\Delta E_{ad} = \Delta E_v - \sum_k \frac{\omega_k}{2}\Delta_k^2$$

In this study, we also present a fragment analysis of the molecular orbitals. It is carried out under the assumption that one can divide the molecular structure into N fragments. The electronic density may then be decomposed and described by means of atomic orbitals centered on nuclei corresponding to the fragments. Fragment contribution is computed as follows:[78]

$$C_{frag} = \sum_j^{n_{frag}} c_j^2 + \sum_j^{n_{frag}} \sum_{i<j}^{n_{frag}} 2c_i c_j S_{ij}$$

where i and j run over the n_{frag} basis set atomic orbitals, c_i is the coefficient by which the basis function enters the molecular orbital, and S_{ij} is the basis set overlap matrix element.

Compound Characterization. All compounds were obtained[22] as described for quinoline derivatives.[49] The reaction yields (after purification) varied between 35 and 45%. The typical procedure was as follows: to the magnetically stirred solution (nitrogen atmosphere) of substituted 1-benzoylmethyleneisoquinoline (1g) in dry chloroform (15−20 mL) and *N*-ethyldiisopropylamine (two equivalents), BF_3 etherate (two equivalents) was added. The solution was stirred overnight at room temperature, and then concentrated Na_2CO_3 water solution(20 mL) was added slowly to the mixture. The organic fraction was separated, the water layer extracted with chloroform (two times using ca. 20−30 mL), dried (Na_2SO_4), and evaporated under reduced pressure. Residual solids were purified by flash chromatography (SiO_2) using acetonitrile (**1**) or DCM (**2**−**8**) as an eluent.

*1-(4-Dimethylamino)benzoylmethyleneisoquinoline Difluoroborate (**1**).* 0.52 g (44.6%). ^{1}H NMR (DMSO-d_6 from TMS) δ: 8.92 (d, 1H, $^3J_{H,H}$ = 8.3 Hz), 8.07 (d, 2H, $^3J_{H,H}$ = 9.0 Hz), 8.02−7.97 (m, 2H), 7.83 (t, 1H), 7.68 (d, 1H, $^3J_{H,H}$ = 6.8 Hz), 7.46 (s, 1H), 6.82 (d, 2H, $^3J_{H,H}$ = 9.0 Hz), 3.06 (s, 6H). ^{11}B NMR (DMSO-d_6 from BF_3·Et_2O) δ: 1.588 (t). ^{13}C NMR (DMSO-d_6 from TMS) δ: 165.8, 152.9, 152.8, 136.5, 134.3, 131.4, 129.5, 129.2, 127.8, 127.3, 123.8, 120.7, 117.8, 111.9, 87.4, ca. 40 (overlapped with solvent signal). ^{15}N (DMSO-d_6 from $MeNO_2$) δ: −196.3. ^{19}F NMR(DMSO-d_6 from $CFCl_3$) δ: −138.3. Mp 260.1−263.8 °C. Anal. Calcd for $C_{19}H_{17}BF_2N_2O$: C, 67.48; H, 5.07; N, 8.28. Found: C, 67.41; H, 5.11; N, 8.20.

*1-(4-Methoxy)benzoylmethyleneisoquinoline Difluoroborate (**2**).* 0.41 g (35.0%). ^{1}H NMR ($CDCl_3$ from TMS) δ: 8.40 (d, 1H, $^3J_{H,H}$ = 8.3 Hz), 8.17 (d, 1H, $^3J_{H,H}$ = 5.4 Hz), 8.04 (d, 2H, $^3J_{H,H}$ = 8.9 Hz), 7.87 (t, 1H), 7.84 (t, 1H), 7.74 (t, 1H), 7.47 (d, 1H, $^3J_{H,H}$ = 6.8 Hz), 7.08 (s, 1H), 6.98 (d, 2H, $^3J_{H,H}$ = 8.9 Hz), 3.89 (s, 3H). ^{11}B NMR ($CDCl_3$ from BF_3·Et_2O) δ: 1.762 (t). ^{13}C NMR δ: 165.9, 162.5, 152.7, 136.6, 133.4, 131.6, 128.9, 128.7, 127.5, 126.8, 125.6, 123.8, 117.8, 114.0, 88.0, 55.5. ^{15}N NMR ($CDCl_3$ from $MeNO_2$) δ: −193.6. ^{19}F NMR ($CDCl_3$ from $CFCl_3$) δ: −139.05. Mp 236.5−238.7 °C. Anal. Calcd for $C_{18}H_{14}BF_2NO_2$: C, 66.50; H, 4.34; N, 4.31. Found: C, 66.39; H, 4.52; N, 4.23.

*1-(4-Methyl)benzoylmethyleneisoquinoline Difluoroborate (**3**).* 0.49 g (41.4%). ^{1}H NMR ($CDCl_3$ from TMS) δ: 8.42 (d, 1H, $^3J_{H,H}$ = 8.4 Hz), 8.21 (d, 1H, $^3J_{H,H}$ = 5.6 Hz), 7.98 (d, 2H, $^3J_{H,H}$ = 8.4 Hz), 7.89 (t, 1H), 7.86 (t, 1H), 7.76 (t, 1H), 7.51 (d, 1H, $^3J_{H,H}$ = 6.8 Hz), 7.30 (d, 2H, $^3J_{H,H}$ = 8.4 Hz), 7.15 (s, 1H), 2.45 (s, 3H). ^{11}B NMR ($CDCl_3$ from BF_3·Et_2O) δ: 1.787 (t). ^{13}C NMR δ: 166.1, 152.7, 142.1, 136.5, 133.4, 131.6, 131.5, 129.3, 128.8, 127.5, 127.0, 125.7, 123.8, 118.1, 88.8, 21.5. ^{15}N NMR ($CDCl_3$ from $MeNO_2$) δ: −192.5. ^{19}F NMR ($CDCl_3$ from $CFCl_3$) δ: −138.7. Mp 231.2−233.5 °C. Anal. Calcd for $C_{18}H_{14}BF_2NO$: C, 69.94; H, 4.56; N, 4.53. Found: C, 69.75; H, 4.71; N, 4.44.

*1-(3-Methyl)benzoylmethyleneisoquinoline Difluoroborate (**4**).* 0.51 g (43.1%). ^{1}H NMR ($CDCl_3$ from TMS) δ: 8.43 (d, 1H, $^3J_{H,H}$ = 8.7 Hz), 8.21 (d, 1H, $^3J_{H,H}$ = 6.8 Hz), 7.90−7.84 (overlapped signals, 4H), 7.76 (t, 1H), 7.52 (d, 1H, $^3J_{H,H}$ = 6.8 Hz), 7.37 (t, 1H), 7.31 (d, 1H, $^3J_{H,H}$ = 7.6 Hz), 7.16 (s, 1H), 2.45 (s, 3H). ^{11}B NMR ($CDCl_3$ from BF_3·Et_2O) δ: 1.800 (t). ^{13}C NMR δ: 166.1, 152.6, 138.4, 136.6, 134.3, 133.5, 132.3, 131.7, 128.9, 128.5, 127.6, 127.5, 125.7, 124.1, 123.8, 118.4, 89.3, 21.4. ^{15}N NMR ($CDCl_3$ from $MeNO_2$) δ: −192.2. ^{19}F NMR ($CDCl_3$ from $CFCl_3$) δ: −138.6. Mp 215.6−218.4 °C. Anal. Calcd for $C_{18}H_{14}BF_2NO$: C, 69.94; H, 4.56; N, 4.53. Found: C, 69.81; H, 4.78; N, 4.49.

*1-Benzoylmethyleneisoquinoline Difluoroborate (**5**).* 0.49 g (41.1%). ^{1}H NMR ($CDCl_3$ from TMS) δ: 8.42 (d, 1H, $^3J_{H,H}$ = 8.5 Hz), 8.22 (d, 1H, $^3J_{H,H}$ = 6.1 Hz), 8.07 (d, 2H, $^3J_{H,H}$ = 8.2 Hz), 7.89 (t, 1H), 7.86 (t, 1H), 7.76 (t, 1H), 7.53 (d, 1H, $^3J_{H,H}$ = 6.8 Hz), 7.51−7.45 (m, 3H), 7.17 (s, 1H). ^{11}B NMR ($CDCl_3$ from BF_3·Et_2O) δ: 1.805 (t). ^{13}C NMR δ: 165.9, 152.6, 136.6, 134.4,133.5, 131.7, 131.5, 128.9, 128.6, 127.5, 126.9, 125.7, 123.8, 118.5, 89.3. ^{15}N NMR ($CDCl_3$ from $MeNO_2$) δ: −195.7. ^{19}F NMR ($CDCl_3$ from $CFCl_3$) δ: −138.6. Mp 233.7−236.8 °C. Anal. Calcd for $C_{17}H_{12}BF_2NO$: C, 69.19; H, 4.10; N, 4.75. Found: C, 69.13; H, 4.06; N, 4.70.

*1-(4-Bromo)benzoylmethyleneisoquinoline Difluoroborate (**6**).* 0.50 g (43.6%). ^{1}H NMR ($CDCl_3$ from TMS) δ: 8.42 (d, 1H, $^3J_{H,H}$ = 8.4 Hz), 8.24 (d, 1H, $^3J_{H,H}$ = 6.8 Hz), 7.94−7.87 (m, 4H), 7.80 (t, 1H), 7.60 (d, 2H, $^3J_{H,H}$ = 8.5 Hz), 7.58 (d, 1H, $^3J_{H,H}$ = 6.6 Hz), 7.16 (s, 1H). ^{11}B NMR ($CDCl_3$ from BF_3·Et_2O) δ:1.750 (t). ^{13}C NMR δ: 164.5, 152.3, 136.7, 133.7, 133.3, 131.9, 131.7, 129.1, 128.4, 127.6, 126.1, 125.6, 123.8, 118.8, 89.5. ^{15}N NMR ($CDCl_3$ from $MeNO_2$) δ: −190.4. ^{19}F NMR ($CDCl_3$ from $CFCl_3$) δ: −138.5. Mp 231.8−234.9 °C. Anal. Calcd for $C_{17}H_{11}BBrF_2NO$: C, 54.60; H, 2.96; N, 3.75. Found: C, 54.53; H, 3.01; N, 3.67.

*1-(3-Bromo)benzoylmethyleneisoquinoline Difluoroborate (**7**).* 0.44 g (38.4%). ^{1}H NMR ($CDCl_3$ from TMS) δ: 8.44 (d, 1H, $^3J_{H,H}$ = 8.3 Hz), 8.25 (d, 1H, $^3J_{H,H}$ = 6.3 Hz), 8.20 (m, 1H), 7.99 (d, 1H, $^3J_{H,H}$ = 8.0 Hz), 7.94−7.86 (m, 2H), 7.80 (t, 1H), 7.63 (d, 1H, $^3J_{H,H}$ = 8.0 Hz), 7.59 (d, 1H, $^3J_{H,H}$ = 6.8 Hz), 7.36 (t, 1H), 7.15 (s, 1H). ^{11}B NMR ($CDCl_3$ from BF_3·Et_2O) δ: 1.748 (t). ^{13}C NMR δ: 164.0, 152.3, 136.7, 136.4, 134.2, 133.7, 131.8, 130.1, 129.8, 129.1, 127.6, 125.7, 125.5, 123.8, 122.9, 119.1, 90.0. ^{15}N NMR ($CDCl_3$ from $MeNO_2$) δ: −189.8. ^{19}F NMR ($CDCl_3$ from $CFCl_3$) δ: −138.5. Mp 227.5−229.2 °C. Anal. Calcd for $C_{17}H_{11}BBrF_2NO$: C, 54.60; H, 2.96; N, 3.75. Found: C, 54.48; H, 3.09; N, 3.68.

DOI: 10.1021/jo502244j
J. Org. Chem. 2015, 80, 2072−2080

*1-(4-Trifluoromethyl)benzoylmethyleneisoquinoline Difluoroborate (**8**).* 0.48 g (41.7%). ^{1}H NMR ($CDCl_3$ from TMS) δ: 8.44 (d, 1H, $^{3}J_{H,H}$ = 8.5 Hz), 8.26 (d, 1H, $^{3}J_{H,H}$ = 6.6 Hz), 8.12 (d, 2H, $^{3}J_{H,H}$ = 8.3 Hz), 7.93 (t, 1H), 7.88 (d, 1H, $^{3}J_{H,H}$ = 7.5 Hz), 7.81 (t, 1H), 7.69 (d, 2H, $^{3}J_{H,H}$ = 8.3 Hz), 7.59 (d, 1H, $^{3}J_{H,H}$ = 6.6 Hz), 7.22 (s, 1H). ^{11}B NMR ($CDCl_3$ from $BF_3{\cdot}Et_2O$) δ: 1.770 (t). ^{13}C NMR δ: 163.6, 152.1, 137.6, 136.7, 133.8, 132.7, 131.7, 129.2, 127.6, 127.0, 125.7, 125.5, 125.14, 123.8, 122.4, 119.4, 90.6. ^{15}N NMR ($CDCl_3$ from $MeNO_2$) δ: −190.5. ^{19}F NMR ($CDCl_3$ from $CFCl_3$) δ: −138.2, −62.9. Mp 230.9−234.2 °C. Anal. Calcd for $C_{18}H_{11}BF_5NO$: C, 59.54; H, 3.05; N, 3.86. Found: C, 59.45; H, 3.14; N, 3.81.

■ ASSOCIATED CONTENT

Supporting Information

NMR spectra, correlation and comparison charts, fluorescence decay spectra, computational results, and Cartesian coordinates. This material is available free of charge via the Internet at http://pubs.acs.org.

■ AUTHOR INFORMATION

Corresponding Author

*E-mail: borys.osmialowski@utp.edu.pl or borys.osmialowski@gmail.com.

Notes

The authors declare no competing financial interest.

■ ACKNOWLEDGMENTS

Financial support from the National Science Centre (Grant No. 2013/09/B/ST5/03550) is gratefully acknowledged. This research was supported by PL-Grid Infrastructure and the Wroclaw Center for Networking and Supercomputing. R.Z. is a Wenner-Gren Foundations scholar.

■ REFERENCES

(1) Loudet, A.; Burgess, K. *Chem. Rev.* **2007**, *107*, 4891.
(2) Boens, N.; Leen, V.; Dehaen, W. *Chem. Soc. Rev.* **2012**, *41*, 1130.
(3) Kamkaew, A.; Lim, S. H.; Lee, H. B.; Kiew, L. V.; Chung, L. Y.; Burgess, K. *Chem. Soc. Rev.* **2013**, *42*, 77.
(4) Nepomnyashchii, A. B.; Bard, A. J. *Acc. Chem. Res.* **2012**, *45*, 1844.
(5) Frath, D.; Massue, J.; Ulrich, G.; Ziessel, R. *Angew. Chem., Int. Ed.* **2014**, *53*, 2290.
(6) Jacquemin, D.; Chibani, S.; Le Guennic, B.; Mennucci, B. *J. Phys. Chem. A* **2014**, *118*, 5343.
(7) Chibani, S.; Laurent, A. D.; Le Guennic, B.; Jacquemin, D. *J. Chem. Theory Comput.* **2014**, *10*, 4574.
(8) Laurent, A. D.; Adamo, C.; Jacquemin, D. *Phys. Chem. Chem. Phys.* **2014**, *16*, 14334.
(9) Nie, S.; Chiu, D. T.; Zare, R. N. *Anal. Chem.* **1995**, *67*, 2849.
(10) Ozdemir, T.; Sozmen, F.; Mamur, S.; Tekinay, T.; Akkaya, E. U. *Chem. Commun.* **2014**, *50*, 5455.
(11) Cao, X.; Lin, W.; Yu, Q.; Wang, J. *Org. Lett.* **2011**, *13*, 6098.
(12) Suzuki, S.; Kozaki, M.; Nozaki, K.; Okada, K. *J. Photochem. Photobiol. C: Photochem. Rev.* **2011**, *12*, 269.
(13) Lin, H.-Y.; Huang, W.-C.; Chen, Y.-C.; Chou, H.-H.; Hsu, C.-Y.; Lin, J. T.; Lin, H.-W. *Chem. Commun.* **2012**, *48*, 8913.
(14) Ooyama, Y.; Hagiwara, Y.; Mizumo, T.; Harima, Y.; Ohshita, J. *RSC Adv.* **2013**, *3*, 18099.
(15) Kubota, Y.; Ozaki, Y.; Funabiki, K.; Matsui, M. *J. Org. Chem.* **2013**, *78*, 7058.
(16) Kubota, Y.; Sakuma, Y.; Funabiki, K.; Matsui, M. *J. Phys. Chem. A* **2014**, *118*, 8717.
(17) Kubota, Y.; Hara, H.; Tanaka, S.; Funabiki, K.; Matsui, M. *Org. Lett.* **2011**, *13*, 6544.
(18) Graser, M.; Kopacka, H.; Wurst, K.; Ruetz, M.; Kreutz, C. R.; Müller, T.; Hirtenlehner, C.; Monkowius, U.; Knör, G.; Bildstein, B. *Inorg. Chim. Acta* **2013**, *405*, 116.
(19) Xia, M.; Wu, B.; Xiang, G. *J. Fluorine Chem.* **2008**, *129*, 402.
(20) Yan, W.; Wan, X.; Chen, Y. *J. Mol. Struct.* **2010**, *968*, 85.
(21) Tokoro, Y.; Nagai, A.; Chujo, Y. *Macromolecules* **2010**, *43*, 6229.
(22) Zhou, Y.; Xiao, Y.; Li, D.; Fu, M.; Qian, X. *J. Org. Chem.* **2008**, *73*, 1571.
(23) Díaz-Moscoso, A.; Emond, E.; Hughes, D. L.; Tizzard, G. J.; Coles, S. J.; Cammidge, A. N. *J. Org. Chem.* **2014**, *79*, 8932.
(24) Li, H.-J.; Fu, W.-F.; Li, L.; Gan, X.; Mu, W.-H.; Chen, W.-Q.; Duan, X.-M.; Song, H.-B. *Org. Lett.* **2010**, *12*, 2924.
(25) Fischer, G. M.; Daltrozzo, E.; Zumbusch, A. *Angew. Chem., Int. Ed.* **2011**, *50*, 1406.
(26) Nagai, A.; Kokado, K.; Nagata, Y.; Arita, M.; Chujo, Y. *J. Org. Chem.* **2008**, *73*, 8605.
(27) Samonina-Kosicka, J.; DeRosa, C. A.; Morris, W. A.; Fan, Z.; Fraser, C. L. *Macromolecules* **2014**, *47*, 3736.
(28) Poon, C.-T.; Lam, W. H.; Wong, H.-L.; Yam, V. W.-W. *J. Am. Chem. Soc.* **2010**, *132*, 13992.
(29) Zhang, G.; St. Clair, T. L.; Fraser, C. L. *Macromolecules* **2009**, *42*, 3092.
(30) Frath, D.; Azizi, S.; Ulrich, G.; Ziessel, R. *Org. Lett.* **2012**, *14*, 4774.
(31) Frath, D.; Azizi, S. b.; Ulrich, G.; Retailleau, P.; Ziessel, R. *Org. Lett.* **2011**, *13*, 3414.
(32) Yu, C.; Jiao, L.; Zhang, P.; Feng, Z.; Cheng, C.; Wei, Y.; Mu, X.; Hao, E. *Org. Lett.* **2014**, *16*, 3048.
(33) Suresh, D.; Gomes, C. S. B.; Gomes, P. T.; Di Paolo, R. E.; Macanita, A. L.; Calhorda, M. J.; Charas, A.; Morgado, J.; Teresa Duarte, M. *J. Chem. Soc. Dalton. Trans.* **2012**, *41*, 8502.
(34) Kertesz, M.; Choi, C. H.; Yang, S. *Chem. Rev.* **2005**, *105*, 3448.
(35) Sobczyk, L.; Grabowski, S. J.; Krygowski, T. M. *Chem. Rev.* **2005**, *105*, 3513.
(36) Raczyńska, E. D.; Kosińska, W.; Ośmiałowski, B.; Gawinecki, R. *Chem. Rev.* **2005**, *105*, 3561.
(37) Cyrański, M. K. *Chem. Rev.* **2005**, *105*, 3773.
(38) Ortí, E.; Viruela, R.; Viruela, P. M. *J. Phys. Chem.* **1996**, *100*, 6138.
(39) Soldatova, A. V.; Kim, J.; Peng, X.; Rosa, A.; Ricciardi, G.; Kenney, M. E.; Rodgers, M. A. J. *Inorg. Chem.* **2007**, *46*, 2080.
(40) Kolehmainen, E.; Ośmiałowski, B.; Krygowski, T. M.; Kauppinen, R.; Nissinen, M.; Gawinecki, R. *J. Chem. Soc. Perkin Trans. 2* **2000**, 1259.
(41) Kolehmainen, E.; Ośmiałowski, B.; Nissinen, M.; Kauppinen, R.; Gawinecki, R. *J. Chem. Soc. Perkin Trans. 2* **2000**, 2185.
(42) Ośmiałowski, B.; Kolehmainen, E.; Nissinen, M.; Krygowski, T. M.; Gawinecki, R. *J. Org. Chem.* **2002**, *67*, 3339.
(43) Krygowski, T. M.; Zachara, J. E.; Ośmiałowski, B.; Gawinecki, R. *J. Org. Chem.* **2006**, *71*, 7678.
(44) Min, J.; Ameri, T.; Gresser, R.; Lorenz-Rothe, M.; Baran, D.; Troeger, A.; Sgobba, V.; Leo, K.; Riede, M.; Guldi, D. M.; Brabec, C. J. *ACS Appl. Mater. Interfaces* **2013**, *5*, 5609.
(45) Gresser, R.; Hummert, M.; Hartmann, H.; Leo, K.; Riede, M. *Chem.—Eur. J.* **2011**, *17*, 2939.
(46) Ni, Y.; Zeng, W.; Huang, K.-W.; Wu, J. *Chem. Commun.* **2013**, *49*, 1217.
(47) Mueller, T.; Gresser, R.; Leo, K.; Riede, M. *Sol. Energy Mater. Sol. C* **2012**, *99*, 176.
(48) Kubo, Y.; Minowa, Y.; Shoda, T.; Takeshita, K. *Tetrahedron Lett.* **2010**, *51*, 1600.
(49) Zakrzewska, A.; Zaleśny, R.; Kolehmainen, E.; Ośmiałowski, B.; Jędrzejewska, B.; Ågren, H.; Pietrzak, M. *Dyes Pigm.* **2013**, *99*, 957.
(50) Yamaguchi, Y.; Matsubara, Y.; Ochi, T.; Wakamiya, T.; Yoshida, Z.-i. *J. Am. Chem. Soc.* **2008**, *130*, 13867.
(51) Goldberg, N. N.; Barkley, L. B.; Levine, R. *J. Am. Chem. Soc.* **1951**, *73*, 4301.

DOI: 10.1021/jo502244j
J. Org. Chem. 2015, 80, 2072−2080

(52) Zakrzewska, A.; Kolehmainen, E.; Valkonen, A.; Haapaniemi, E.; Rissanen, K.; Chęcińska, L.; Ośmiałowski, B. *J. Phys. Chem. A* **2012**, *117*, 252.
(53) Xu, S.; Evans, R. E.; Liu, T.; Zhang, G.; Demas, J. N.; Trindle, C. O.; Fraser, C. L. *Inorg. Chem.* **2013**, *52*, 3597.
(54) Yu, Y.-H.; Descalzo, A. B.; Shen, Z.; Röhr, H.; Liu, Q.; Wang, Y.-W.; Spieles, M.; Li, Y.-Z.; Rurack, K.; You, X.-Z. *Chem.—Asian J.* **2006**, *1*, 176.
(55) Hecht, M.; Fischer, T.; Dietrich, P.; Kraus, W.; Descalzo, A. B.; Unger, W. E. S.; Rurack, K. *ChemistryOpen* **2013**, *2*, 25.
(56) Bura, T.; Retailleau, P.; Ulrich, G.; Ziessel, R. *J. Org. Chem.* **2011**, *76*, 1109.
(57) Ono, M.; Watanabe, H.; Kimura, H.; Saji, H. *ACS Chem. Neurosci.* **2012**, *3*, 319.
(58) Lager, E.; Liu, J.; Aguilar-Aguilar, A.; Tang, B. Z.; Peña-Cabrera, E. *J. Org. Chem.* **2009**, *74*, 2053.
(59) Angulo, G.; Grampp, G.; Rosspeintner, A. *Spectrochim. Acta, Part A* **2006**, *65*, 727.
(60) Birks, J. B.; Dyson, D. J. *Proc. R. Soc. A* **1963**, *275*, 135.
(61) Grabowski, Z. R.; Rotkiewicz, K.; Rettig, W. *Chem. Rev.* **2003**, *103*, 3899.
(62) Wiggins, P.; Williams, J. A. G.; Tozer, D. J. *J. Chem. Phys.* **2009**, *131*, 091101.
(63) Guido, C. A.; Mennucci, B.; Jacquemin, D.; Adamo, C. *Phys. Chem. Chem. Phys.* **2010**, *12*, 8016.
(64) Barfield, M.; Fagerness, P. *J. Am. Chem. Soc.* **1997**, *119*, 8699.
(65) Laurent, A. D.; Jacquemin, D. *Int. J. Quantum Chem.* **2013**, *113*, 2019.
(66) Jacquemin, D.; Perpète, E. A.; Ciofini, I.; Adamo, C.; Valero, R.; Zhao, Y.; Truhlar, D. G. *J. Chem. Theory Comput.* **2010**, *6*, 2071.
(67) Silva-Junior, M. R.; Schreiber, M.; Sauer, S. P. A.; Thiel, W. *J. Chem. Phys.* **2008**, *129*, 104103.
(68) Chibani, S.; Le Guennic, B.; Charaf-Eddin, A.; Laurent, A. D.; Jacquemin, D. *Chem. Sci.* **2013**, *4*, 1950.
(69) Le Guennic, B.; Chibani, S.; Charaf-Eddin, A.; Massue, J.; Ziessel, R.; Ulrich, G.; Jacquemin, D. *Phys. Chem. Chem. Phys.* **2013**, *15*, 7534.
(70) Chibani, S.; Charaf-Eddin, A.; Le Guennic, B.; Jacquemin, D. *J. Chem. Theory Comput.* **2013**, *9*, 3127.
(71) Er, J. C.; Tang, M. K.; Chia, C. G.; Liew, H.; Vendrell, M.; Chang, Y.-T. *Chem. Sci.* **2013**, *4*, 2168.
(72) Jin, J.-L.; Li, H.-B.; Geng, Y.; Wu, Y.; Duan, Y.-A.; Su, Z.-M. *ChemPhysChem* **2012**, *13*, 3714.
(73) Chibani, S.; Le Guennic, B.; Charaf-Eddin, A.; Maury, O.; Andraud, C.; Jacquemin, D. *J. Chem. Theory Comput.* **2012**, *8*, 3303.
(74) Cammi, R.; Mennucci, B. *J. Chem. Phys.* **1999**, *110*, 9877.
(75) Chibani, S.; Budzak, S.; Medved, M.; Mennucci, B.; Jacquemin, D. *Phys. Chem. Chem. Phys.* **2014**, *16*, 26024.
(76) Frisch, M. J.; Trucks, G. W.; Schlegel, H. B.; Scuseria, G. E.; Robb, M. A.; Cheeseman, J. R.; Scalmani, G.; Barone, V.; Mennucci, B.; Petersson, G. A.; Nakatsuji, H.; Caricato, M.; Li, X.; Hratchian, H. P.; Izmaylov, A. F.; Bloino, J.; Zheng, G.; Sonnenberg, J. L.; Hada, M.; Ehara, M.; Toyota, K.; Fukuda, R.; Hasegawa, J.; Ishida, M.; Nakajima, T.; Honda, Y.; Kitao, O.; Nakai, H.; Vreven, T.; Montgomery, J. J. A. ; Peralta, J. E.; Ogliaro, F.; Bearpark, M.; Heyd, J. J.; Brothers, E.; Kudin, K. N.; Staroverov, V. N.; Kobayashi, R.; Normand, J.; Raghavachari, K.; Rendell, A.; Burant, J. C.; Iyengar, S. S.; Tomasi, J.; Cossi, M.; Rega, N.; Millam, J. M.; Klene, M.; Knox, J. E.; Cross, J. B.; Bakken, V.; Adamo, C.; Jaramillo, J.; Gomperts, R.; Stratmann, R. E.; Yazyev, O.; Austin, A. J.; Cammi, R.; Pomelli, C.; Ochterski, J. W.; Martin, R. L.; Morokuma, K.; Zakrzewski, V. G.; Voth, G. A.; Salvador, P.; Dannenberg, J. J.; Dapprich, S.; Daniels, A. D.; Farkas, O.; Foresman, J. B.; Ortiz, J. V.; Cioslowski, J.; Fox, D. J. *Gaussian 09*, revision A.02; Gaussian, Inc.: Wallingford CT, 2009.
(77) Petrenko, T.; Neese, F. *J. Chem. Phys.* **2007**, *127*, 164319.
(78) Savarese, M.; Aliberti, A.; De Santo, I.; Battista, E.; Causa, F.; Netti, P. A.; Rega, N. *J. Phys. Chem. A* **2012**, *116*, 7491.

DOI: 10.1021/jo502244j
J. Org. Chem. 2015, 80, 2072−2080